

Diameter dependence of the growth velocity of silicon nanowires synthesized via the vapor-liquid-solid mechanism

V. Schmidt,* S. Senz, and U. Gösele

Max-Planck-Institut für Mikrostrukturphysik, Weinberg 2, D-06120 Halle, Germany

(Received 29 September 2006; revised manuscript received 30 November 2006; published 24 January 2007)

We present a model for the radius dependence of the growth velocity of Si nanowires synthesized via the vapor-liquid-solid mechanism. By considering the interplay of the Si incorporation and crystallization rate at steady state conditions we show that the radius dependence of the growth velocity in general depends on the derivatives of the incorporation and crystallization velocity with respect to the supersaturation. Taking this into account, the apparently contradictory experimental observations regarding the radius dependence of the growth velocity can be reconciled and explained consistently.

DOI: 10.1103/PhysRevB.75.045335

PACS number(s): 68.65.-k, 81.05.Cy, 81.10.Bk

INTRODUCTION

Despite the recent progress made in semiconductor nanowire research¹⁻⁶ the vapor-liquid-solid (VLS) growth mechanism, by which most of the nanowires are synthesized today, is not yet fully understood. In particular, one technologically important issue, the diameter dependence of the nanowire growth velocity, has not been satisfactorily addressed so far. In this paper a thermodynamic model dealing mainly with the diameter dependence of the nanowire growth velocity is presented. On the basis of this model other important effects like the correlation between pressure dependence and diameter dependence of the growth velocity are also discussed.

One issue that is intimately connected with the diameter dependence of the growth velocity is the question of the rate-determining step of the VLS growth mechanism. The question of the rate-determining step is a very fundamental one and essential in understanding the VLS mechanism. The VLS mechanism is schematically depicted in Fig. 1(a) exemplarily for the chemical vapor deposition of Si nanowires. In this case the VLS mechanism can be divided into three main steps [see Fig. 1(a)]:

- (i) the incorporation step [comprising the adsorption and cracking of the Si precursor at the surface of the liquid metal-Si alloy droplet, leading to a supply of Si at a rate ρ_{in} (mol/s)];
- (ii) the diffusion step [describing the diffusion of Si through the droplet];
- (iii) the crystallization step [characterizing the growth of Si nanowire at the liquid-solid interface, proceeding at a rate ρ_{cr} (mol/s)].

Especially in the 1970s several authors⁷⁻⁹ discussed which of these three steps is rate determining for VLS growth, and just recently this topic was brought up again.¹⁰ The outcome of this discussion was that the diffusion step presumably does not affect the growth rate, since Si diffusion through a microscopic liquid droplet is too fast as to be rate determining.¹¹ Mainly in view of the pressure dependence of the growth velocity (see, e.g., Refs. 7, 8, 12, and 13), Bootsma and Gassen⁸ argued that the incorporation step must be the rate-determining one. In contrast to this, based on the dependence of growth velocity on the crystallographic orientation of the wires, Givargizov¹¹ argued that the crystal-

lization step determines the growth rate. The question, however, of whether the assumption of a single rate-determining step is valid at all has not been raised. In view of the arguments in favor of step (i) or (iii), we suggest that the assumption of a single rate-determining steps has to be rejected. Instead, a model of the VLS mechanism has to consider the interplay of both the incorporation and the crystallization steps in order to account for the different experimentally observed effects. Deriving such a model and investigating its implications for the diameter dependences of the growth velocity and the supersaturation of the droplet is the aim of this paper.

DEFINITIONS

To start with, several chemical potentials (CPs) and chemical potential (CP) differences are to be defined [see Fig. 1(b)]. Although not indicated explicitly in the following discussion, all CPs are meant to be CPs of Si. The CP of the substrate, μ_0^s , fixed by the boundary conditions, is taken as a reference point. We assume that the incorporation rate $\rho_{in}(p, \mu^{vl})$ depends on both the pressure p and the CP difference between vapor and liquid, $\mu^{vl} = \mu^v - \mu^l$. The pressure dependence is related to the fact that statistically more precursor gas molecules will hit the droplet surface when the absolute value of the pressure is increased, whereas the μ^{vl} dependence is related to the probability that the precursor gas

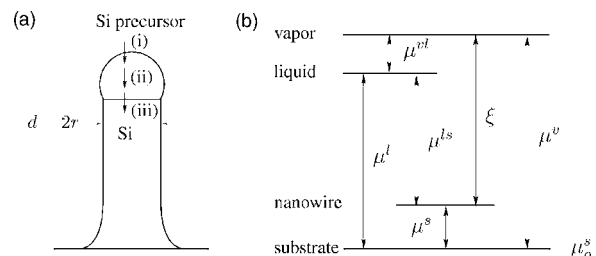


FIG. 1. (a) Schematic of the VLS mechanism: (i) incorporation, (ii) diffusion, (iii) crystallization. (b) Chemical potentials (CPs): μ_0^s =CP of the Si substrate, μ^v =CP of the Si vapor, μ^s =CP of the Si nanowire (NW), μ^{vl} =CP difference between vapor and liquid, μ^{ls} =CP difference between liquid and Si NW, ξ =CP difference between vapor and Si NW.

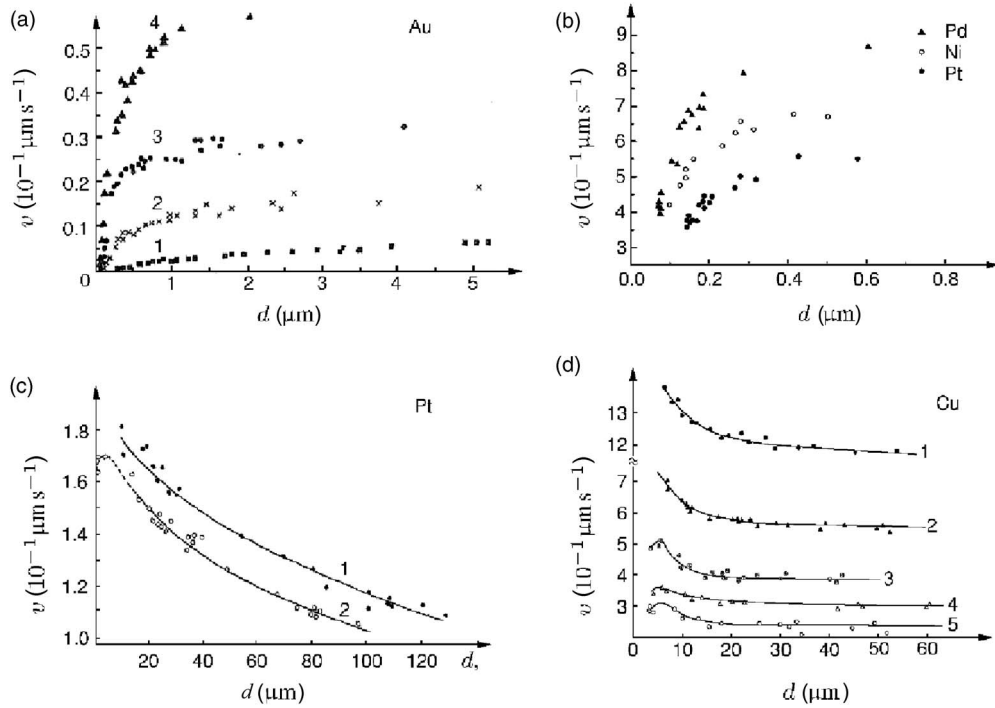


FIG. 2. Diameter dependence of the growth velocity; all experiments performed with SiCl_4 as precursor. (a) Growth velocity v as a function of the wire diameter d ; SiCl_4 pressure increases from (1) to (4); after Ref. 7. (b) v as a function of d ; $1130\text{ }^\circ\text{C}$; $\text{SiCl}_4/\text{H}_2=6.7\%$; after Ref. 7. (c) v as a function of d ; temperature $1000\text{--}1100\text{ }^\circ\text{C}$; (1) $\text{SiCl}_4:\text{H}_2=0.9\%$, (2) 0.95% ; after Ref. 9. (d) v as a function of d ; temperature (1) 1027 , (2) 1047 , (3) 1067 , (4) 1087 , and (5) $1107\text{ }^\circ\text{C}$; after Ref. 14.

molecules will stick on the droplet surface and will be cracked into their constituents. As shown in Fig. 1(b), ξ , the CP difference between vapor and nanowire, can be expressed as $\xi = \mu^v - \mu^s = \mu^{vl} + \mu^{ls}$. The crystallization rate $\rho_{cr}(\mu^{ls})$ is assumed to depend on the droplet supersaturation $\mu^{ls} = \mu^l - \mu^s$, i.e., the CP difference between liquid, μ^l , and nanowire, μ^s . Due to the surface contribution to the Gibbs free energy, the CP of the nanowire becomes greater than the CP of the substrate, μ_0^s . This is the so-called Gibbs-Thomson effect. Keeping in mind that μ^s was defined with μ_0^s as its reference point [see Fig. 1(b)], this gives

$$\mu^s = \frac{C^s}{r}, \quad (1)$$

where C^s is defined as $C^s = 2\Omega^s\sigma^s$, with Ω^s and σ^s being the molar volume and the surface tension of silicon, respectively. The Gibbs-Thomson effect causes the growth velocity to be diameter dependent.

EXPERIMENTAL RESULTS

The diameter dependence of the growth velocity of silicon nanowires has been investigated by several groups.^{7,9,10,14–16} In Fig. 2 the experimental results of Givargizov⁷ [Figs. 2(a) and 2(b)], Weyher⁹ [Fig. 2(c)] and Nebol'sin *et al.*¹⁴ [Fig. 2(d)] are reproduced. All data shown in Fig. 2 have been obtained in silicon wire growth experiments performed at high temperatures around $1000\text{ }^\circ\text{C}$ using SiCl_4 as precursor gas.

Three important experimental results, which we now want to address one, by one can be deduced from the collection of data sets shown in Fig. 2.

The first and maybe most important result is that oppositional diameter dependencies can be observed [compare Figs. 2(a) and 2(b) with Figs. 2(c) and 2(d)]. In Figs. 2(a) and 2(b) the results of Givargizov⁷ can be seen. They show an increase of the growth velocity with increasing diameter using different catalyst materials [Au in Fig. 2(a), Pt, Ni, and Pd in Fig. 2(b)]. Givargizov⁷ explained the observed increase of the growth velocity with increasing diameter by a decrease of μ^s according to Eq. (1), leading to an increase of the supersaturation $\mu^{ls} = \mu^l - \mu^s$ of the droplet with respect to the nanowire. Since the supersaturation is the driving force of the crystallization process, an increase of the supersaturation should cause an increase of the growth velocity. In contrast to this, Weyher⁹ using Pt [see Fig. 2(c)] and Nebol'sin *et al.*¹⁴ using Cu as catalyst [see Fig. 2(d)] observed the opposite diameter dependence—a decrease of the growth velocity with increasing diameter. This surprising outcome is still in want of a sound explanation. In any case, it demonstrates that the diameter dependence of the growth velocity is a more complex phenomenon than usually expected. Since different catalysts have been used in Fig. 2 one is tempted to explain the differences in the observed behavior by the differences in the catalyst material. However, this does not provide a satisfactory explanation as the Pt results of Fig. 2(b) show the opposite behavior to the Pt results of Fig. 2(c). Thus differences in the catalyst cannot account for the effect.

The second important outcome of the data shown in Fig. 2 is that a correlation between the pressure dependence and the

diameter dependence seems to exist. The data sets of Fig. 2(a) show an increase of the growth velocity with increasing pressure [in Fig. 2 the pressure is increased from data set 1 to 4]. At the same time an increase of the growth velocity with increasing diameter can be seen in Fig. 2(a). So the growth velocity can be augmented either by a pressure or by a diameter increase. This is the usual and expected behavior and we refer to it in the following as the normal behavior. The data sets of Fig. 2(c), on the other hand, show the opposite characteristic. Here the growth velocity decreases if either the pressure or the radius is increased [in Fig. 2(c) the pressure increases from data set 1 to 2]. A decrease of the growth velocity with increasing pressure is somehow counterintuitive and we therefore refer to it as the anomalous behavior. It is important to note that in both cases, the normal one of Fig. 2(a) and the anomalous one of Fig. 2(c), a pressure increase has the same effect on the growth velocity as a diameter increase. Thus the diameter and pressure dependence seem to be correlated.

We have not discussed Fig. 2(d) yet, wherein the diameter dependence is shown for various growth temperatures. One can see in Fig. 2(d) that the growth velocity decreases as the growth temperature is increased, which is as odd as the pressure dependence shown in Fig. 2(c). Since increasing the temperature, like increasing the pressure, augments the supply of silicon (due to the higher precursor gas cracking efficiency), the data in Fig. 2(d) support the validity of the anomalous pressure dependence shown in Fig. 2(c). To test whether an anomalous pressure dependence indeed coincides with an anomalous temperature dependence would be a very interesting and worthwhile experiment.

The third outcome of Fig. 2 is that a maximum of the growth velocity seems to be present at a radius of approximately $10 \mu\text{m}$ as indicated for some of the graphs of Figs. 2(c) and 2(d). It is interesting to note that the assumption of a maximum of the growth velocity is not in contradiction to the behavior shown in Figs. 2(a) and 2(b), since here the growth velocity has only been determined for radii smaller than $\approx 5 \mu\text{m}$. To summarize, from the data presented in Fig. 2 three non trivial results can be derived: (1) opposite diameter dependencies can be found in different VLS silicon nanowire growth experiments, (2) a correlation between the radius and the pressure dependence seems to exist, and (3) the growth velocity, at least in some cases, exhibits a maximum.

THEORY

The first assumption of our model is that growth proceeds via the VLS mechanism and that silicon is supplied directly from the gas phase to the droplet. Hence the surface diffusion of silicon is neglected, which is a valid assumption at the extremely high growth velocities of Fig. 2. Furthermore, we assume that the diffusion of silicon through the droplet is sufficiently fast so that the diffusion process can be neglected and that we therefore can concentrate on the interplay of the crystallization and incorporation processes. Clearly, the incorporation rate $\rho_{in}(p, \mu^{vl})$ of Si atoms is proportional to the surface area of the droplet, which in turn is proportional to

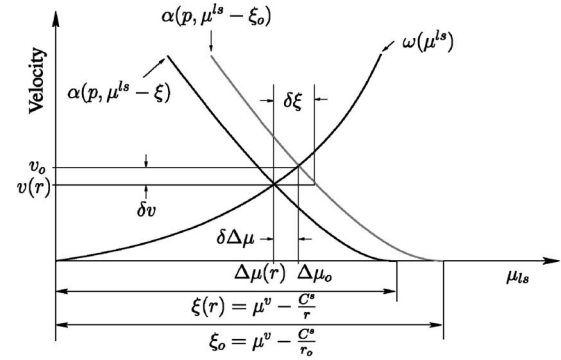


FIG. 3. Schematic of the incorporation velocity $\alpha(p, \mu^{ls} - \xi)$ and the crystallization velocity $\omega(\mu^{ls})$ as a function of the droplet supersaturation nanowire μ^{ls} ; $\alpha(p, \mu^{ls} - \xi)$ is given for two different radii, r_0 (gray curve) and r .

the cross section πr^2 of the nanowire. Thus by dividing $\rho_{in}(p, \mu^{vl})$ by πr^2 and multiplying with Ω^s we can define the incorporation velocity

$$\alpha(p, \mu^{vl}) = \rho_{in}(p, \mu^{vl}) \frac{\Omega^s}{\pi r^2}, \quad (2)$$

which is taken to be radius independent for constant μ^{vl} and constant pressure. In a similar way, we can define the crystallization velocity

$$\omega(\mu^{ls}) = \rho_{cr}(\mu^{ls}) \frac{\Omega^s}{\pi r^2}. \quad (3)$$

Also $\omega(\mu^{ls})$ is assumed to be radius independent for constant μ^{ls} . It is obvious that under steady state conditions the incorporation rate has to equal the crystallization rate. By using $\mu^{vl} = \xi - \mu^{ls}$ we obtain

$$\rho_{cr}(\mu^{ls}) = \rho_{in}(p, \xi - \mu^{ls})|_{\mu^{ls} = \Delta\mu}. \quad (4)$$

This condition defines the steady state supersaturation $\Delta\mu$ and the steady state growth velocity $v = \omega(\Delta\mu) = \alpha(p, \xi - \Delta\mu)$.

For simplicity we assume that the crystallization velocity $\omega(\mu^{ls})$ is a monotonically increasing function of μ^{ls} . Similarly, we assume that the incorporation velocity is a monotonically increasing function of μ^{vl} , i.e., the CP difference between vapor and liquid. Using the identity $-\mu^{vl} = \mu^{ls} - \xi$, we can plot both velocities in one graph as functions of the supersaturation μ^{ls} , where, due to the minus sign, the α curve is flipped with respect to the vertical axis. This is schematically shown in Fig. 3 where the incorporation velocity $\alpha(p, \mu^{ls} - \xi)$ and the crystallization velocity $\omega(\mu^{ls})$ are displayed as functions of the supersaturation μ^{ls} .

Furthermore we assume that the incorporation rate becomes zero if the CP difference between vapor and liquid becomes zero. This defines the x -axis intercept $\mu^{ls} = \xi$ of the α curve, assuming that $\alpha(\mu^{ls} = \xi) = 0$ is equivalent to neglecting the CP difference caused by the cracking of the precursor molecule. Including the energetics of the chemical reaction, however, will only shift the x -axis intercept by an additional constant term, which does not affect the further analysis.

In a steady state situation $\alpha(p, \mu^{ls} - \xi)$ has to equal $\omega(\mu^{ls})$. The intersection point of the gray α curve in Fig. 3 with the ω curve thus defines the values of the steady state supersaturation $\Delta\mu_0$ and of the steady state growth velocity v_0 for this specific radius r_0 .

Though at an early stage of the analysis, we can already figure out what caused the experimentally observed correlation between the pressure and the radius dependence [see Figs. 2(a) and 2(c)]. Considering the x -axis intercept of the α curve given by $\mu^v - C^s/r$ one can see that both a pressure increase and a radius increase will cause an increase of the x -axis intercept. In both cases the α curve will be shifted to the right, effecting similar changes of steady state growth velocity. Therefore we can expect the pressure dependence to be correlated with the diameter dependence.

Such a correlation between the pressure and the radius dependence is not only nontrivial, it might also be significant from a technical point of view. In order to accurately adjust the lengths of Si nanowires (having a certain diameter variation) it is helpful if the diameter dependence of the growth velocity is as small as possible. Due to the correlation between the pressure and the diameter dependence, the regime where the diameter dependence is minimal should coincide with the regime where the pressure dependence (for the diameter in question) is minimal. Thus, by choosing the proper growth pressure, the length variation of the nanowires could be minimized.

Let us come back to Fig. 3 and consider a situation where the radius is decreased from r_0 to r . This will cause the α curve to be shifted to smaller μ^{ls} values by an amount $\delta\xi = C^s/r_0 - C^s/r$. If $\delta\xi$ is sufficiently small, i.e., considering large radii, we can locally expand $\alpha(p, \mu^{ls} - \xi)$ and $\omega(\mu^{ls})$ in a Taylor series expansion to first order around the intersection point at $\mu^{ls} = \Delta\mu_0$:

$$\omega(\mu^{ls}) = \omega_0 + \omega_1(\mu^{ls} - \Delta\mu_0),$$

$$\alpha(p, \mu^{ls} - \xi) = \alpha_0 + \alpha_1[(\mu^{ls} - \Delta\mu_0) - (\xi - \xi_0)], \quad (5)$$

where $\alpha_1 = \partial\alpha/\partial\mu^{ls}|_{\mu^{ls}=\Delta\mu_0}$ and $\omega_1 = \partial\omega/\partial\mu^{ls}|_{\mu^{ls}=\Delta\mu_0}$ are the slopes at $\mu^{ls} = \Delta\mu_0$. Using the steady state conditions [$\mu^{ls} = \Delta\mu$, $\omega_0 = \alpha_0 = v_0$, and $\omega(\Delta\mu) = \alpha(p, \Delta\mu - \xi)$] we can solve for $\Delta\mu$. If additionally $r_0 = \infty$ is taken as the starting point of the expansion we can use $\xi - \xi_0 = -C^s/r$ and $\Delta\mu_0 = \mu_0^l$, and we end up with the following expressions for the steady state supersaturation:

$$\Delta\mu = \mu_0^l + \frac{\alpha_1}{\omega_1 - \alpha_1} \frac{2\Omega^s \sigma^s}{r} \quad (6)$$

and the steady state growth velocity

$$v = v_0 + \frac{\omega_1 \alpha_1}{\omega_1 - \alpha_1} \frac{2\Omega^s \sigma^s}{r}. \quad (7)$$

One can see that as a consequence of the Gibbs-Thomson effect both the steady state supersaturation and the steady state growth velocity become radius dependent. But what is more important is that both magnitude and sign of the radius-dependent terms in Eqs. (6) and (7) depend on the sign and magnitude of the slopes α_1 and ω_1 of the α and ω curves,

respectively. Thus by considering the interplay between the incorporation and the crystallization steps we could derive an expression for the steady state growth velocity which allows for both types of diameter dependencies—an increase or a decrease of the growth velocity with increasing radius. This is the most important outcome of our model.

DISCUSSION

With respect to the values of α_1 and ω_1 , different cases have to be considered.

Different limits

Let us first discuss the limits mentioned in the beginning, where either the incorporation step or the crystallization step determines the growth velocity.

(1) A situation where the incorporation step is rate determining corresponds to the limit $\omega_1 \rightarrow \infty$. In this limit, the steady state growth velocity becomes

$$v = v_0 + \alpha_1 \frac{2\Omega^s \sigma^s}{r}. \quad (8)$$

Considering the usual situation where the incorporation rate increases with increasing pressure, i.e., $\alpha_1 < 0$, an increase of the growth velocity with increasing radius can be expected.

(2) In the other limit, $\alpha_1 \rightarrow \infty$, corresponding to a situation where the crystallization step is rate determining, the steady state supersaturation becomes

$$\Delta\mu = \mu_0^l - \frac{2\Omega^s \sigma^s}{r}. \quad (9)$$

Note that this equation agrees with the one derived by Givargizov⁷ under the assumption that the crystallization step is rate determining. So the outcome of our model is consistent with his considerations. This, on the other hand, shows that the formula of Givargizov is not generally valid and can only be applied in the limit where the crystallization step is rate determining. This is of crucial importance as the formula of Givargizov is often applied without discussing its limited range of validity. In this limit ($\alpha_1 \rightarrow \infty$), the steady state growth velocity is given by

$$v = v_0 - \omega_1 \frac{2\Omega^s \sigma^s}{r}, \quad (10)$$

which, supposing $\omega_1 > 0$, signifies a velocity increase with increasing radius. Thus in both limits discussed above, assuming $\alpha_1 < 0$ and $\omega_1 > 0$, an increase of the growth velocity with increasing radius is expected. So a discussion on which step is the rate-determining one cannot account for the complex behavior shown in Fig. 2.

(3) Our model might also be applied to the case where the incorporation rate is independent of the supersaturation, i.e., $\alpha_1 \rightarrow 0$. As pointed out by Kodambaka *et al.*¹⁰ this might be the cause for the radius independence of the growth velocity they observed in their experiments using disilane as precursor at very low pressures (10^{-8} – 10^{-5} Torr). One can see from Eq. (7) that the radius dependence of the growth veloc-

ity indeed vanishes, if the incorporation rate is taken to be independent of the supersaturation ($\alpha_1 \rightarrow 0$).

Signs of α_1 : Different cases

According to Eq (7), the nature of the diameter dependence depends on the signs of α_1 and ω_1 . By introducing the factor

$$\Gamma \equiv \frac{\omega_1 \alpha_1}{\omega_1 - \alpha_1} \quad (11)$$

Eq. (7) can be written as

$$v = v_0 + \Gamma \frac{2\Omega^s \sigma^s}{r}. \quad (12)$$

If we assume that the crystallization velocity ω is a monotonic function with positive slope ω_1 , we have to distinguish two cases.

(1) The first case applies to $\alpha_1 < 0$, for which Γ becomes negative. According to Eq. (12) the steady growth velocity increases with increasing radius. This would correspond to the experimentally observed behavior presented in Figs. 2(a) and 2(b).

(2) In the second case, $\omega_1 > \alpha_1 > 0$, Γ is positive. Thus according to Eq. (12) the growth velocity would decrease with increasing radius, in accordance with the data of Weyher⁹ and Nebol'sin *et al.*¹⁴ presented in Figs. 2(c) and 2(d).

So the character of the radius dependence changes if the incorporation velocity changes its sign. Such a sign change is possible if the incorporation velocity α exhibits a maximum, a scenario which we now want to consider in more detail.

Maximum of the growth velocity

The third experimental finding was that some of the data sets displayed in Figs. 2(c) and 2(d) seem to show a maximum of the growth velocity. Such a maximum of the growth velocity can be described in terms of our model if we assume as a hypothesis that also the incorporation velocity $\alpha(p, \mu^{ls} - \xi)$ exhibits a maximum. Supposing that this maximum of the α curve is sufficiently smooth so that it can be approximated in the vicinity of the maximum by a parabola, and supposing that a linear approximation of the ω curve is sufficiently accurate in the vicinity of the intersection point $\Delta\mu_0$, then the following expression for the steady state growth velocity v can be derived:

$$v(r) = v_0 + \frac{\omega_1}{2\alpha_2} \left[\omega_1 + 2\alpha_2 \left(\frac{C^s}{r_0} - \frac{C^s}{r} \right) - \sqrt{\omega_1^2 + 4\alpha_2\omega_1 \left(\frac{C^s}{r_0} - \frac{C^s}{r} \right)} \right], \quad (13)$$

with $\alpha_2 = \partial^2 \alpha / \partial (\mu^{ls})^2|_{\mu^{ls}=\Delta\mu_0}$ being the curvature of the α curve, and r_0 and v_0 being the radius and the growth velocity of the maximum.

In Fig. 4, the function of Eq. (13) is fitted to data set 2 of Fig. 2(c) by using the values of r_0 , v_0 , σ^s ,¹⁷ and Ω^s as input

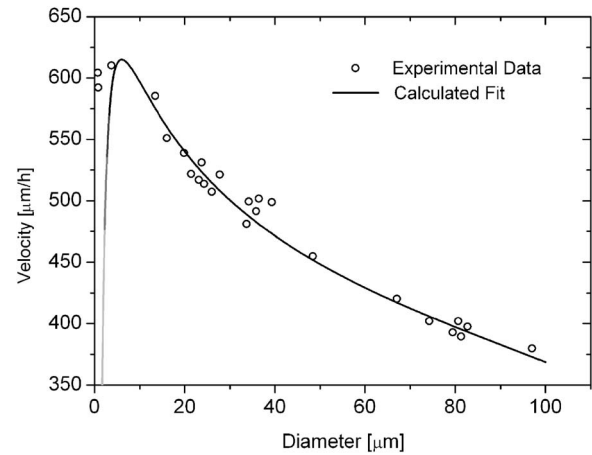


FIG. 4. Data set 2 of Fig. 2(c) after Weyher (Ref. 9) and calculated fit using Eq. (13) and the following parameters: $C^s = 30 \text{ J mol}^{-1} \mu\text{m}$, $r_0 = 3 \mu\text{m}$, $v_0 = 615 \mu\text{m h}^{-1}$, $\omega_1 = 33.6 \mu\text{m h}^{-1} \text{ mol J}^{-1}$, $\alpha_2 = -0.88 \mu\text{m h}^{-1} \text{ mol}^2 \text{ J}^{-2}$.

and ω_1 and α_2 as fit parameters (see the caption of Fig. 4). As shown in Fig. 4 the calculated steady state growth velocity shows good agreement with experiment. Only for radii smaller than r_0 does the calculated velocity curve show a sharp decrease and does not properly reproduce the experimental data. This is because in deriving Eq. (13), we assumed that we can approximate the α curve in the vicinity of its maximum by a parabola. However, due to the $1/r$ dependence of the supersaturation, this approximation becomes invalid if the radius is considerably smaller than r_0 . This decreased validity of Eq. (13) is indicated in Fig. 4 by the fading out of the curve.

Finally, we would like to remark that our results cannot be directly applied to growth experiments where the Si supply itself is strongly radius dependent, such as, for example, in the case of the molecular beam epitaxy,^{18,19} or the metal-organic vapor phase epitaxy of nanowires.²⁰

CONCLUSION

In conclusion, considering the interplay of the incorporation step at the catalyst surface and the crystallization step, we derived a model for the radius dependence of the steady state growth velocity v . It is found that the radius dependence of v depends on the derivatives of the incorporation and crystallization velocities with respect to the supersaturation μ^{ls} , which explains apparently contradictory experimental observations. Furthermore, our model explains the origin for the experimentally observed correlation between the radius dependence and the pressure dependence. Several limits of our model were discussed. Finally, by assuming a maximum of the incorporation velocity, we could derive an analytical expression for v , which, if fitted to the experimental data, shows good agreement.

ACKNOWLEDGMENTS

This work was partially funded by the EU Project No. NODE 015783.

*Electronic address: vschmidt@mpi-halle.de

- ¹J. B. Hannon, S. Kodambaka, F. M. Ross, and R. M. Tromp, *Nature (London)* **440**, 69 (2006).
- ²J. Goldberger, A. I. Hochbaum, R. Fan, and P. Yang, *Nano Lett.* **6**, 973 (2006).
- ³C. Yang, Z. Zhong, and C. M. Lieber, *Science* **310**, 1304 (2005).
- ⁴Q. Tang, T. I. Kamins, X. Liu, D. E. Grupp, and J. S. Harris, *Electrochem. Solid-State Lett.* **8**, G205 (2005).
- ⁵H. Pettersson, J. Trägårdh, A. I. Perrson, L. Landin, D. Hessman, and L. Samuelson, *Nano Lett.* **6**, 229 (2006).
- ⁶V. Schmidt, H. Riel, S. Senz, S. Karg, W. Riess, and U. Gösele, *Small* **2**, 85 (2006).
- ⁷E. I. Givargizov, *J. Cryst. Growth* **31**, 20 (1975).
- ⁸G. A. Bootsma and H. J. Gassen, *J. Cryst. Growth* **10**, 223 (1971).
- ⁹J. Weyher, *J. Cryst. Growth* **43**, 235 (1978).
- ¹⁰S. Kodambaka, J. Tersoff, M. C. Reuter, and F. M. Ross, *Phys. Rev. Lett.* **96**, 096105 (2006).
- ¹¹E. I. Givargizov, *Highly Anisotropic Crystals* (Reidel, Dordrecht, 1987), pp. 119–125.
- ¹²J. Westwater, D. P. Gosain, S. Tomiya, and S. Usui, *J. Vac. Sci. Technol. B* **15**, 554 (1997).
- ¹³K.-K. Lew and J. M. Redwing, *J. Cryst. Growth* **254**, 14 (2003).
- ¹⁴V. A. Nebol'sin, A. A. Shchetinin, A. A. Dolgachev, and V. V. Korneeva, *Inorg. Mater.* **41**, 1256 (2005).
- ¹⁵Y. Wu, R. Fan, and P. Yang, *Nano Lett.* **2**, 83 (2002).
- ¹⁶J. Kikkawa, Y. Ohno, and S. Takeda, *Appl. Phys. Lett.* **86**, 123109 (2006).
- ¹⁷R. J. Jaccodine, *J. Electrochem. Soc.* **110**, 524 (1963).
- ¹⁸L. Schubert, P. Werner, N. D. Zakharov, G. Gerth, F. M. Kolb, L. Long, and U. Gösele, *Appl. Phys. Lett.* **84**, 4968 (2004).
- ¹⁹V. G. Dubrovskii, N. V. Sibirev, G. E. Cirlin, J. C. Harmand, and V. M. Ustinov, *Phys. Rev. E* **73**, 021603 (2006).
- ²⁰J. Johansson, C. P. T. Svensson, T. Mårtensson, L. Samuelson, and W. Seifert, *J. Phys. Chem. B* **109**, 13567 (2005).